NASA TECHNICAL NOTE

NASA TN D-2654

NASA TN D-2654

A MODIFIED METHOD OF INTEGRAL RELATIONS FOR SUPERSONIC NONEQUILIBRIUM FLOW OVER A WEDGE

by Perry A. Newman

Langley Research Center
Langley Station, Hampton, Va.

NATIONAL AERONAUTICS AND SPACE ADMINISTRATION • WASHINGTON, D. C. • FEBRUARY 1965

A MODIFIED METHOD OF INTEGRAL RELATIONS FOR SUPERSONIC NONEQUILIBRIUM FLOW OVER A WEDGE

By Perry A. Newman

Langley Research Center
Langley Station, Hampton, Va.

NATIONAL AERONAUTICS AND SPACE ADMINISTRATION

For sale by the Office of Technical Services, Department of Commerce,
Washington, D.C. 20230 -- Price $2.00

A MODIFIED METHOD OF INTEGRAL RELATIONS FOR SUPERSONIC NONEQUILIBRIUM FLOW OVER A WEDGE

By Perry A. Newman
Langley Research Center

SUMMARY

The standard method of integral relations has been modified so that better results are obtained for inviscid nonequilibrium supersonic flow over wedges. The polynomial profiles assumed for certain integrands in the standard method are not used. Instead, the definite integral itself is replaced by an expression in which the values of the integrand at the upper and lower limits are weighted to account for the nonequilibrium effects. These weighting functions are computed by considering relaxation histories along frozen-flow streamlines. Conversion of the partial differential flow equations to ordinary equations using weighting functions is no more laborious than in the standard method.

The resulting approximate system is integrated smoothly from the frozen-flow shock values to the equilibrium asymptotic values. The entropy layer on the wedge surface is not predicted by the approximate system but results from integration of a set of corrected equations. Numerical results are presented for vibrational relaxation of a pure diatomic gas (nitrogen) and dissociation relaxation of the Lighthill-Freeman "ideal dissociating gas" (oxygen). These particular cases have been selected so that a comparison can be made with existing characteristics calculations. The results are also compared with those of the standard method of integral relations as well as with those of a recent perturbation solution.

INTRODUCTION

The method of integral relations is a numerical method for solving systems of nonlinear partial differential equations by transforming them to approximate systems of ordinary differential equations. This method and its applications have been reviewed recently by Belotserkovskiy and Chushkin in reference 1 which gives a very good description of the method as well as an extensive bibliography. Two recent applications of the method to nonequilibrium flow have appeared in the literature. South (refs. 2 and 3) has considered the vibrational relaxation of a pure diatomic gas over wedges and cones, while Shih, et al. (ref. 4) have considered the chemical relaxation of air (5 species) over a blunt body. Other methods which have been used to compute nonequilibrium

flow over pointed bodies include the method of characteristics (for example, refs. 5 to 8) and perturbation methods (ref. 9).

The obvious advantage of the integral methods is that highly efficient techniques for solving ordinary differential equations have been developed for high-speed digital computers. Results given in references 2 and 3 as well as those reported herein were computed in less than 5 minutes per case on an IBM 7090 electronic data processing system. The major disadvantage is lack of detail within the shock layer. The other methods mentioned previously also have their limitations. As is pointed out in reference 6, application of the method of characteristics to nonequilibrium problems is not straightforward; furthermore, the computation time can be very long, even on high-speed computers. The major difficulty with the perturbation method is in application to problems of practical interest - that is, one is interested in dissociation phenomena, for example, only if dissociation is significant; then the perturbation is no longer small. Lee (ref. 9) carefully delineates the conditions under which his perturbation solution is valid.

In applying the standard method of integral relations (defined in ref. 1 as the simple method) to nonequilibrium flow past wedges and cones, South (ref. 2) found that the asymptotic value (far from the tip) of the surface vibrational energy did not converge as the order of the approximation increased. The surface nonequilibrium rate equation of the approximate system caused erroneous overshoots or undershoots of about equal magnitude in the asymptotic value of this energy. Reference 2 indicates that this phenomenon was due to the existence of three distinct zones in the shock layer far from the tip: (1) a relaxation zone just behind the shock wave, (2) an equilibrium zone in the interior, and (3) an entropy layer next to the body surface. The thicknesses of zones (1) and (3), relative to that of the entire shock layer, get smaller with distance from the tip but they do not vanish - that is, the shock boundary condition of frozen flow remains, even though most of the shock layer is in equilibrium. Thus, profiles of flow variables across the shock layer approach discontinuities and cannot be adequately approximated by low-order polynomials.

The idea of the present modification is to replace integrals across the shock layer with an expression in which the values of the integrand at the shock wave and on the wedge surface are weighted to account for the nonequilibrium effects. In general, these functions are determined by considering the relaxation history along frozen-flow streamlines - that is, the shock geometry (shock angle and streamline positions), as well as the pressure and velocity, is taken as if the flow were frozen for the determination of the weighting functions. These functions depend on the distance along the surface from the wedge tip. In the standard method, an equal weight is given to each strip boundary and this weighting is not altered with distance downstream.

In order to test the method, two cases using different gas models have been computed. In the first, hereafter called gas I, vibrational relaxation in a pure diatomic gas is considered. The second, hereafter called gas II, is the Lighthill-Freeman "ideal dissociating gas" (refs. 10 and 11).

SYMBOLS

Primed quantities are dimensional; unprimed quantities are nondimensional. (See eqs. (7), (8), and (9).) Suffix I on an equation number indicates that the equation applies only to gas I, while the suffix II applies only to gas II.

a nonequilibrium weighting function (see eq. (18))

C_1 vibrational nonequilibrium rate parameter

C_2 dissociation nonequilibrium rate parameter

c_p frozen-flow specific heat at constant pressure

E vibrational energy

E_{eq} equilibrium vibrational energy

F defined by equation (15)

$g = p + \rho u^2$

$h = \rho v$

$H = p + \rho v^2$

K dissociation energy per mole of the diatomic species divided by the product of T'_∞ and the molar gas constant for the diatomic species

K_i functions defined in appendix B

L' nonequilibrium length scale

M frozen-flow Mach number

p pressure

P, Q defined by equation (15)

$\overline{Q}$ defined by equation (19)

S dissociation nonequilibrium rate parameter

$t = \rho u$

T temperature

u,v	velocity components in x- and y-direction, respectively
V	total velocity
x,y	coordinate along and normal to wedge surface, respectively
$z = \rho uv$	
α	degree of dissociation, mass fraction of atoms
β	shock-wave angle
γ	ratio of frozen-flow specific heats
δ	shock-layer thickness in y-direction
ϵ	vibrational nonequilibrium driving force
θ	wedge half-angle
Θ_v	characteristic vibrational temperature
λ	shock-layer included angle, $\beta - \theta$
ξ	dummy variable for x
ρ	density
ρ_D	characteristic density of dissociation
τ	vibrational relaxation time
ϕ	dissociation nonequilibrium driving force

Subscripts:

0	quantity evaluated at surface ($y = 0$)
c	corrected surface quantity
i	index
w	quantity used in determination of weighting functions
W	initial value ($x = 0$) of w subscripted quantity
∞	free-stream quantity
δ	quantity evaluated at shock wave ($y = \delta$)

$( )_0$ quantity evaluated at the tip ($x = 0$, $y = 0$), that is, initial value

Bars over symbols indicate average values.

PROBLEM DEFINITION

General Description

The problem to be discussed is the steady supersonic flow of a pure diatomic gas past wedges at zero incidence. The shock wave is attached and the flow is inviscid and isoenergetic with only one dissipative mechanism. Two different gas models are considered; in the first (gas I) the dissipative mechanism is the vibrational relaxation. The second (gas II) is the Lighthill-Freeman "ideal dissociating gas" (refs. 10 and 11) where the dissipative mechanism is the dissociation relaxation.

The results for gas I can be directly compared with the standard method results given in reference 2 and the characteristics results given in reference 5. For gas II, the results for both the standard and modified methods are presented herein. These results are compared with the characteristics results of reference 7.

Basic Equations

The geometry and coordinate system are pictured in figure 1 and are identical to those used in reference 2. The basic flow and rate equations are written as (ref. 3, specialized for the wedge)

Continuity:

$$\frac{\partial}{\partial x}(\rho u) + \frac{\partial}{\partial y}(\rho v) = 0 \qquad (1)$$

x-momentum:

$$\frac{\partial}{\partial x}(\rho u^2 + p) + \frac{\partial}{\partial y}(\rho uv) = 0 \qquad (2)$$

y-momentum:

$$\frac{\partial}{\partial x}(\rho uv) + \frac{\partial}{\partial y}(\rho v^2 + p) = 0 \qquad (3)$$

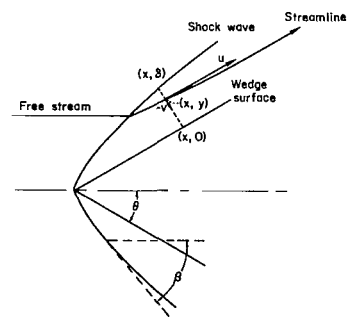

Figure 1.- Geometry and coordinate system for nonequilibrium flow.

Rate:

$$\frac{\partial}{\partial x}(\rho u E) + \frac{\partial}{\partial y}(\rho v E) - \rho\epsilon = 0 \tag{4.I}$$

$$\frac{\partial}{\partial x}(\rho u \alpha) + \frac{\partial}{\partial y}(\rho v \alpha) - \rho\phi = 0 \tag{4.II}$$

where E is the nondimensionalized vibrational energy, α is the degree of dissociation, and ϵ and ϕ are the nonequilibrium driving forces for gases I and II, respectively.

The energy and state equations for gases I and II are

Energy:

$$T + E + \frac{1}{5} M_\infty{}^2(u^2 + v^2) = 1 + \frac{1}{5} M_\infty{}^2 \tag{5.I}$$

$$\left(1 + \frac{\alpha}{4}\right)T + \frac{K}{4}\alpha + \frac{1}{6} M_\infty{}^2(u^2 + v^2) = 1 + \frac{1}{6} M_\infty{}^2 \tag{5.II}$$

State:

$$\frac{7}{5} M_\infty{}^2 p = \rho T \tag{6.I}$$

$$\frac{4}{3} M_\infty{}^2 p = (1 + \alpha)\rho T \tag{6.II}$$

The free-stream ratios of frozen-flow specific heats γ_∞ of 7/5 for gas I and 4/3 for gas II have been used in equations (5) and (6). It should be noted that $\gamma = 4/3$ for gas II (when $\alpha = 0$) because of the manner in which the vibrational-energy mode is treated. (See ref. 10.)

Quantities have been nondimensionalized as follows (primes denote dimensional quantities):

$$\left.\begin{aligned} u,v &= \frac{(u',v')}{V_\infty'} \qquad p = \frac{p'}{\rho_\infty' V_\infty'^2} \qquad \rho = \frac{\rho'}{\rho_\infty'} \\ T &= \frac{T'}{T_\infty'} \qquad x,y = \frac{(x',y')}{L'} \end{aligned}\right\} \tag{7}$$

The quantity E is nondimensionalized as $E = \dfrac{E'}{c_p' T_\infty'}$.

As in references 2 and 5, the length scale L' for gas I is taken to be

$$L' = V'_\infty \tau'(0,0) \tag{8.I}$$

where $\tau'(0,0)$ is the vibrational relaxation time on the surface at the tip. Also τ' and the driving force ϵ are given as

$$\left.\begin{aligned} p'\tau' &\propto \exp\left[\left(\frac{C_1}{T'}\right)^{1/3}\right] \\ \epsilon &= \frac{(E_{eq} - E)}{\tau} \\ \tau &= \frac{\tau'}{\tau'(0,0)} \\ E_{eq} &= \frac{2}{7}\left(\frac{\Theta'_v}{T'_\infty}\right)\left[\exp\left(\frac{\Theta'_v}{T'_\infty}\frac{1}{T}\right) - 1\right]^{-1} \end{aligned}\right\} \tag{9.I}$$

The quantity C_1 is an experimentally determined rate parameter, Θ'_v is the characteristic vibrational temperature, and E_{eq} is the equilibrium value of E for the temperature T. As in reference 5, C_1 was determined from the data of Blackman (ref. 12).

For gas II, the length scale L' is taken as that given in reference 7 as

$$L' = V'_\infty \frac{\rho'_D}{\rho'_\infty}\frac{T'_\infty S}{\rho'_\infty C_2} \tag{8.II}$$

where C_2 is the C of references 7 and 11. (Note, however, that reference 7 does not use this length scale.) As in references 7 and 11, the driving force ϕ is then taken to be

$$\phi = \rho_D \rho T^{-S}\left[(1 - \alpha)e^{-K/T} - \frac{\rho}{\rho_D}\alpha^2\right] \tag{9.II}$$

The quantities C_2 and S are experimentally determined rate parameters while ρ'_D is the characteristic density of dissociation defined by Lighthill

(ref. 10). Note that when the quantity within the brackets of equation (9.II) vanishes, the equilibrium condition is obtained (ref. 10). As in reference 7, C_2 and S were taken from the data of Matthews (ref. 13) for oxygen.

Boundary Conditions

The boundary conditions are those given in reference 2. There it is assumed that the free-stream nonequilibrium energy variable is zero and that it remains zero as the flow passes through the shock wave. That is

$$E(x,\delta) = E_\delta(x) = E_\infty = 0 \tag{10.I}$$

$$\alpha(x,\delta) = \alpha_\delta(x) = \alpha_\infty = 0 \tag{10.II}$$

Thus the frozen-flow shock-wave relations apply and all quantities immediately behind the shock wave are functions of γ_∞, M_∞, θ, and $\beta(x)$. These relations, taken from reference 14, are given in appendix A. Since $\beta(x)$ is the only x-dependent quantity in a shock function $f(x,\delta) \equiv f_\delta(x)$, then

$$\frac{df_\delta}{dx} = \frac{df_\delta}{d\beta}\frac{d\beta}{dx} \tag{11}$$

Further, the shock wave is attached at the tip, so that

$$\delta(0) = 0 \tag{12}$$

The location of the shock wave downstream is obtained from

$$\frac{d\delta}{dx} = \tan\lambda \tag{13}$$

where $\lambda = \beta - \theta$. Finally, the surface is a streamline so that

$$v(x,0) = v_0(x) = 0 \tag{14}$$

APPROXIMATE INTEGRAL SOLUTION

General Equations

The method of integral relations converts a system of nonlinear partial differential equations, such as equations (1) to (4), to an approximate set of nonlinear ordinary differential equations which can be integrated numerically. Equations (1) to (4) are in the divergence or conservation form. That is

$$\frac{\partial Q_i(x,y)}{\partial x} + \frac{\partial P_i(x,y)}{\partial y} - F_i(x,y) = 0 \qquad (i = 1,2,3,4) \qquad (15)$$

Equations (15) are integrated across the shock layer, $y = 0$ to $\delta(x)$, to obtain

$$\frac{d}{dx}\int_0^{\delta(x)} Q_i(x,y)dy - Q_i(x,\delta)\frac{d\delta(x)}{dx} + \left[P_i(x,\delta) - P_i(x,0)\right] - \int_0^{\delta(x)} F_i(x,y)dy = 0 \qquad (16)$$

where Leibnitz's rule for differentiation under the integral sign has been used. In the standard method, polynomial profiles in y are assumed for the quantities $Q_i(x,y)$ and $F_i(x,y)$. For the one-strip approximation with a linear profile (ref. 3), equations (16) become

$$\delta\left(\frac{d}{dx}Q_{i,0} + \frac{d}{dx}Q_{i,\delta}\right) + \left(Q_{i,0} - Q_{i,\delta}\right)\frac{d\delta}{dx} - 2\left(P_{i,0} - P_{i,\delta}\right) - \delta\left(F_{i,0} + F_{i,\delta}\right) = 0 \qquad (17)$$

where $Q_{i,0} = Q_i(x,0)$, etc. Equations analogous to (17) are given for the two- and three-strip approximations in reference 2.

In the modified method presented herein, the integrals in equations (16) are replaced by

$$\int_0^{\delta(x)} Q_i(x,y)dy = \delta(x)\left\{\left[1 - a_i(x)\right]Q_{i,0} + a_i(x)Q_{i,\delta}\right\} \qquad (18)$$

where a_i is the nonequilibrium weighting function for Q_i. With $\overline{Q}_i(x)$ defined as

$$\overline{Q}_i(x) \equiv \frac{1}{\delta(x)} \int_0^{\delta(x)} Q_i(x,y)dy \tag{19}$$

a_i is obtained as

$$a_i(x) = \frac{\overline{Q}_i(x) - Q_{i,0}}{Q_{i,\delta} - Q_{i,0}} \tag{20}$$

In the next section, it is shown how the values of a_i are computed by using equations (19) and (20). With the integrals in equations (16) replaced by equations (18), equations (1) to (4) are transformed to the following approximate ordinary differential equations:

$$\delta\left(1 - a_1\right)\frac{dt_0}{dx} + \delta a_1 \frac{dt_\delta}{dx} - \delta\left(t_0 - t_\delta\right)\frac{da_1}{dx} + \left(1 - a_1\right)\left(t_0 - t_\delta\right)\tan\lambda + h_\delta = 0 \tag{21}$$

$$\delta\left(1 - a_2\right)\frac{dg_0}{dx} + \delta a_2 \frac{dg_\delta}{dx} - \delta\left(g_0 - g_\delta\right)\frac{da_2}{dx} + \left(1 - a_2\right)\left(g_0 - g_\delta\right)\tan\lambda + z_\delta = 0 \tag{22}$$

$$\delta a_3 \frac{dz_\delta}{dx} + \delta z_\delta \frac{da_3}{dx} - \left(1 - a_3\right)z_\delta \tan\lambda + H_\delta - p_0 = 0 \tag{23}$$

$$\delta\left(1 - a_4\right)\frac{d\left(t_0E_0\right)}{dx} - \delta t_0E_0 \frac{da_4}{dx} + \left(1 - a_4\right)t_0E_0 \tan\lambda - \delta\left(1 - a_5\right)\rho_0\epsilon_0 - \delta a_5\rho_\delta\epsilon_\delta = 0 \tag{24.I}$$

$$\delta\left(1 - a_4\right)\frac{d\left(t_0\alpha_0\right)}{dx} - \delta t_0\alpha_0 \frac{da_4}{dx} + \left(1 - a_4\right)t_0\alpha_0 \tan\lambda - \delta\left(1 - a_5\right)\rho_0\phi_0 - \delta a_5\rho_\delta\phi_\delta = 0 \tag{24.II}$$

where

$$\left.\begin{aligned} t &= \rho u \\ h &= \rho v \\ g &= \rho u^2 + p \\ H &= \rho v^2 + p \\ z &= \rho uv \end{aligned}\right\} \tag{25}$$

and a_5, the weighting function for the driving force, is given by equations (18) to (20) where F_i replaces Q_i. Equations (11) and (23) immediately give the differential equation for β. Equations (21), (23), and (24) give the differential equation for E_0 or α_0. In order to separate the differential equations for p_0 and u_0, the energy and state equations ((5) and (6)) must be differentiated and used with equations (21) to (24). The four separated equations used in the numerical integration are given in appendix B.

Determination of the Weighting Functions

The nonequilibrium weighting functions a_i are determined by integrating the streamline rate equation along the frozen-flow (or even equilibrium-flow) streamlines. The frozen-flow solution is the oblique shock solution (appendix A) where

$$\left.\begin{aligned} p_0 &= p_\delta \equiv p_W \\ v_0 &= v_\delta = 0 \\ u_0 &= u_\delta \equiv u_W \\ \rho_0 &= \rho_\delta \equiv \rho_W \\ \beta &\equiv \beta_W \\ E_0 &= E_\delta = 0 \\ \alpha_0 &= \alpha_\delta = 0 \end{aligned}\right\} \tag{26}$$

The shock wave is straight and the streamlines are parallel to the wedge surface. The surface streamline rate equation (valid for all values of x) is

obtained by substitution of equation (1) into equation (4) and application of the surface boundary condition (eq. (14)) and is

$$\frac{dE_0}{dx} = \frac{\epsilon_0}{u_0} \tag{27.I}$$

or

$$\frac{d\alpha_0}{dx} = \frac{\phi_0}{u_0} \tag{27.II}$$

Assumptions.- In reference 5 it is shown that for vibrational relaxation, integration of the surface streamline rate equation with the velocity held constant gave energy and temperature results which compared favorably with the characteristics results. Thus in determining the weighting functions, it is first assumed (for both gas models) that the velocity is constant ($u = u_w$; $v = 0$); this means that the pressure is also constant ($p = p_w$). And second, the departure of the streamlines and shock wave from straight lines due to nonequilibrium effects is neglected. Thus (see fig. 2)

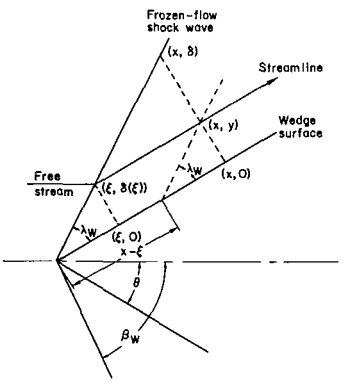

Figure 2.- Geometry and coordinate system for determination of weighting functions.

$$\delta(x) = x \tan \lambda_w \tag{28}$$

In the determination of $\bar{Q}(x)$, it is assumed that a quantity $Q(x,y)$ depends only on the distance along the streamline from the shock wave to the point (x,y), that is (see fig. 2)

$$Q(x,y) = Q(x - \xi, 0) = Q_0(x - \xi) \tag{29}$$

since in frozen flow, the surface streamline is like all other streamlines. Also it can be seen from figure 2 that

$$y = \delta(\xi) = \xi \tan \lambda_w \tag{30}$$

The integral over y in equation (19) can be made into an integral over ξ by using equations (28) to (30). Then

$$\bar{Q}_i(x) = \frac{1}{x} \int_0^x Q_{i,0}(x - \xi) d\xi \tag{31}$$

Now define x'' as $x'' = x - \xi$ and equations (31) become

$$\overline{Q}_i(x) = \frac{1}{x} \int_0^x Q_{i,0}(x'')dx'' \tag{32}$$

Equations.- With the approximations of the previous section, the values of a_i defined in equations (18) are computed from equations (20) as

$$a_1(x) = a_2(x) = a_3(x) = \frac{\overline{\rho}(x) - \rho_w(x)}{\rho_W - \rho_w(x)} \tag{33}$$

and

$$\left.\begin{aligned} a_4(x) &= \frac{\overline{\rho E}(x) - \rho_w(x)E_w(x)}{-\rho_w(x)E_w(x)} \\ a_5(x) &= \frac{\overline{\rho \epsilon}(x) - \rho_w(x)\epsilon_w(x)}{\rho_W \epsilon_W - \rho_w(x)\epsilon_w(x)} \end{aligned}\right\} \tag{34.I}$$

or

$$\left.\begin{aligned} a_4(x) &= \frac{\overline{\rho \alpha}(x) - \rho_w(x)\alpha_w(x)}{-\rho_w(x)\alpha_w(x)} \\ a_5(x) &= \frac{\overline{\rho \phi}(x) - \rho_w(x)\phi_w(x)}{\rho_W \phi_W - \rho_w(x)\phi_w(x)} \end{aligned}\right\} \tag{34.II}$$

The quantities with the subscript w indicate that the quantities are computed along frozen-flow (or equilibrium-flow) streamlines and are functions of either E_W or α_W, which are defined from equations (27) as

$$\frac{dE_w(x)}{dx} \equiv \frac{\epsilon_w(x)}{u_W} \tag{35.I}$$

with

$$\left.\begin{aligned} T_w(x) &\equiv 1 + \frac{M_\infty^2}{5}\left(1 - u_w^2\right) - E_w(x) \\ \rho_w(x) &\equiv \frac{7}{5}\frac{M_\infty^2 p_w}{T_w(x)} \end{aligned}\right\} \qquad (36.I)$$

where τ_w, $E_{eq,w}$, and ϵ_w are given by equations (9.I) with $T = T_w$ for gas I and

$$\frac{d\alpha_w(x)}{dx} \equiv \frac{\phi_w(x)}{u_w} \qquad (35.II)$$

with

$$\left.\begin{aligned} T_w(x) &\equiv \frac{4 + \frac{2}{3}M_\infty^2\left(1 - u_w^2\right) - K\alpha_w(x)}{4 + \alpha_w(x)} \\ \rho_w(x) &\equiv \frac{4M_\infty^2 p_w}{3\left[1 + \alpha_w(x)\right]T_w(x)} \\ \phi_w(x) &\equiv \rho_D\rho_w(x)T_w^{-S}(x)\left\{\left[1 - \alpha_w(x)\right]e^{-\frac{K}{T_w(x)}} - \frac{\rho_w(x)}{\rho_D}\alpha_w^2(x)\right\} \end{aligned}\right\} \qquad (36.II)$$

for gas II. The quantities with the subscript W are the initial values ($x = 0$) of the w subscripted quantities. The barred quantities in equations (33) and (34) are computed from equations (32) where $Q_{i,0}(x'') = Q_{i,w}(x'')$. It was found that $\frac{da_i}{dx}$ was computed accurately enough as

$$\frac{da_i}{dx} = \frac{a_i(x + \Delta x) - a_i(x)}{\Delta x} \qquad (37)$$

Tip Region

It can be seen from the computational equations given in appendix B that the derivatives appear to be unbounded at the tip ($x = 0$) because the shock wave is attached, that is, $\delta(0) = 0$. Since these derivatives are linearly dependent on K_i and the coefficients of K_i do not vanish as $x \to 0$, the necessary condition that a regular solution exists at the tip is $K_i(0) = 0$. When the equations for K_i are set equal to zero, it can be seen that the frozen-flow oblique shock solution is obtained independent of the values of the nonequilibrium weighting functions $a_i(0)$ - that is, $f_0(0) = f_\delta(0)$. Thus the equations of appendix A and the energy and state equations ((5) and (6)) give the tip (or initial) solution.

In order to get the initial derivatives, the quantities $\lim_{x\to 0}\left(\frac{K_i}{\delta}\right)$ must be evaluated. The initial values of a_i will be required. It is shown in appendix C that the initial value of all a_i is $1/2$. The initial derivatives are obtained in appendix D. It can be seen that for gas I, these are the same as those obtained by South in reference 3 (see eqs. (35) to (39) of ref. 3) where it is pointed out that these derivatives are the exact wedge-tip gradients derived by Sedney (ref. 15).

Asymptotic Behavior

Far from the tip, most of the shock layer will be in equilibrium so that the weighting functions, defined by equations (18) to (20), will be changing very little with x. Thus

$$\lim_{x\to\infty}\left(\frac{da_i}{dx}\right) = 0 \tag{38}$$

Furthermore, since $Q_{i,\delta} \neq Q_{i,0}$ and $\bar{Q}_i \to Q_{i,0}$, equation (20) gives

$$\lim_{x\to\infty}\left(a_i\right) = 0 \tag{39}$$

With equations (38) and (39) substituted into the equations of appendix B it can be seen that the derivatives of p_0, u_0, and E_0 (or α_0) go to zero since $\delta \to \infty$ as $x \to \infty$. It is not immediately obvious that $d\beta/dx$ tends to zero because of the presence of the factor δa_3 in the denominator of equation (B9). However, it can be shown (by using a mean value theorem for definite integrals) that

$$\left.\begin{aligned} \lim_{x\to\infty}\left(\frac{1}{a_3}\frac{da_3}{dx}\right) &= 0 \\ \lim_{x\to\infty}\left(\delta a_3\right) &= \text{Constant} \end{aligned}\right\} \tag{40}$$

Thus $d\beta/dx$ will vanish as $x \to \infty$ if the condition

$$\lim_{x\to\infty}\left(K_3\right) = 0 \tag{41}$$

is satisfied.

If the derivatives of the flow variables t_0 and g_0 had been taken with respect to $\ln x$ instead of x, the physical situation would still require these derivatives to vanish as $x \to \infty$, since an equilibrium condition will be reached. Then K_1 and K_2 should also have to approach zero as $x \to \infty$ before the system would stop driving. The simultaneous numerical solution of this asymptotic condition

$$\lim_{x\to\infty}\left(K_1\right) = \lim_{x\to\infty}\left(K_2\right) = \lim_{x\to\infty}\left(K_3\right) = 0 \tag{42}$$

together with the equilibrium condition and the state and energy equations gives the same surface properties and shock angle as those obtained from the equilibrium-flow solution behind an equilibrium shock wave. It is expected then that the modified integral method will give the frozen-flow solution in the tip region and the equilibrium solution for the surface properties and shock angle far downstream.

As was indicated in the "Introduction," the standard method as applied by South (ref. 2) gave rise to unrealistic asymptotic values for the vibrational energy. The asymptotic form of the surface rate equation for the one-strip approximation from reference 2 can be written as

$$\lim_{x\to\infty}\left(\frac{dE_0}{dx}\right) = \frac{\epsilon_0}{u_0} + \frac{\rho_\delta \epsilon_\delta}{\rho_0 u_0} \tag{43.I}$$

The shock-wave driving force ϵ_δ is always positive. Thus the surface driving force ϵ_0 must assume unrealistic negative values before $\lim_{x\to\infty}\left(\frac{dE_0}{dx}\right) = 0$ as it should when an equilibrium condition is reached. The corresponding equation from the modified method is the asymptotic form of equation (B10.I)

$$\lim_{x \to \infty} \left(\frac{dE_0}{dx} \right) = \frac{\epsilon_0}{u_0} \tag{44.I}$$

Note that this is the exact surface rate equation as given by equation (27.I). For equilibrium, ϵ_0 is identically zero.

Corrected Equations

It was shown previously that the exact surface rate equations are given by equation (27). Likewise from equations (1), (2), and (14) the exact surface momentum equation (for all x) is

$$\frac{du_0}{dx} = \frac{-1}{t_0} \frac{dp_0}{dx} \tag{45}$$

With the shock angle and pressure distribution obtained from the equations of appendix B, the exact equations (27) and (45) were integrated (as auxiliary equations to the approximate set of appendix B) in order to obtain the corrected surface properties, defined as

$$\frac{du_c}{dx} \equiv - \frac{1}{t_c} \frac{dp_0}{dx} \tag{46}$$

and for gas I,

$$\frac{dE_c}{dx} \equiv \frac{\epsilon_c}{u_c} \tag{47.I}$$

with

$$\left.\begin{aligned} T_c &\equiv 1 + \frac{M_\infty^2}{5}\left(1 - u_c^2\right) - E_c \\ \rho_c &\equiv \frac{7}{5} \frac{M_\infty^2 p_0}{T_c} \end{aligned}\right\} \tag{48.I}$$

where τ_c, $E_{eq,c}$, and ϵ_c are given by equations (9.I) with $T = T_c$. For gas II the corresponding equations are

$$\frac{d\alpha_c}{dx} \equiv \frac{\phi_c}{u_c} \tag{47.II}$$

with

$$\left.\begin{aligned} T_c &\equiv \frac{4 + \frac{2}{3} M_\infty{}^2\left(1 - u_c{}^2\right) - K\alpha_c}{4 + \alpha_c} \\ \rho_c &\equiv \frac{4M_\infty{}^2 p_0}{3(1 + \alpha_c)T_c} \\ \phi_c &\equiv \rho_D \rho_c T_c{}^{-S}\left[\left(1 - \alpha_c\right)e^{-\frac{K}{T_c}} - \frac{\rho_c}{\rho_D}\alpha_c{}^2\right] \end{aligned}\right\} \tag{48.II}$$

As South points out in reference 2, it is tempting to replace equations (B10) and (B11) with equations (27) and (45), respectively. However, it was found that such a hybrid system either did not integrate stably or had worse asymptotes than the approximate system. Belotserkovskiy and Chushkin (ref. 1) indicate that extraneous equations may appear during the construction of the approximate set and state that these extraneous equations must be more accurately satisfied with increasing approximations (more strips). In this sense then, the corrected equations (46) and (47) are integrated (in addition to the approximate set) in order to get better surface values and to check the approximate set. It will be seen that the entropy-layer effects are obtained from these equations.

Numerical Integration

The approximate system of ordinary differential equations of appendix B, the corrected equations (46) and (47), and frozen streamline rate equations (35) were integrated on an IBM 7090 data processing system using a first-order Euler scheme. The first integration step (using initial derivatives of appendix D) was large (relative to successive steps) in order to get away from the tip indeterminacy. Results for both cases were computed in less than 5 minutes.

When gas II, the Lighthill-Freeman model (refs. 10 and 11), was used, it was found that a hyperbolic stability criterion (for supersonic flow) had to be applied for a stable integration. South (ref. 2) also found that this criterion had to be applied when higher approximations were made in the standard integral method for gas I.

For the one-strip approximation used herein, data are known at the shock wave and on the wedge surface at a given value of x. The intersection of the

right-running characteristic from the shock point and the left-running characteristic from the surface point determines the maximum step size which can be used for a stable integration. (See fig. 3.) For parallel streamlines and constant local Mach number, the geometry (fig. 3) gives

$$\Delta x \leqq \frac{\delta}{2}\left(M_0^2 - 1\right)^{1/2} \tag{49}$$

Figure 5 of reference 2 shows the effect of this stability criterion for a two-strip (standard integral method) integration. This same behavior was found in the one-strip modified method reported herein.

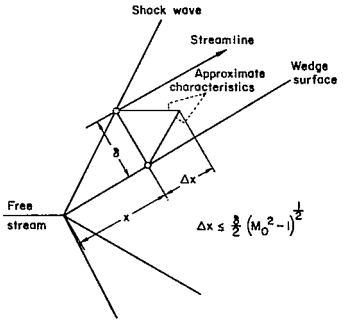

Figure 3.- Approximate hyperbolic stability criterion.

RESULTS AND DISCUSSION

In order to assess the accuracy of the modified integral method the two cases for which characteristics results are available (refs. 5 and 7) have been selected. Case I is for vibrational relaxation in pure nitrogen (gas I) and case II is for the Lighthill-Freeman (refs. 10 and 11) ideal dissociating gas model using constants for oxygen (gas II). Case I has been calculated by using the standard integral method in references 2 and 3. A recent perturbation solution has also been compared (ref. 9).

The parameters for case I are:

$$\theta = 40.02^\circ$$

$$M_\infty = 6$$

$$T'_\infty = 300^\circ \text{ K}$$

$$\frac{\Theta'_v}{T'_\infty} = 11.12$$

$$\frac{C_1}{T'_\infty} = 0.4655 \times 10^4$$

Those for case II are:

$$\theta = 25.175^\circ$$

$$M_\infty = 32$$

$$T'_\infty = 281.24^\circ \text{ K}$$

$$p'_\infty = 1.33389 \times 10^{-3} \text{ atm}$$

$$K = 211.136$$

$$C_2 = 3.5489 \times 10^{23} \frac{(^\circ K)^S cm^3}{g \text{ sec}}$$

$$S = 2.5$$

$$\rho'_D = 150 \text{ g/cm}^3$$

Case II is the same as case I of reference 7 and corresponds to oxygen at about 150,000 feet altitude.

Vibrational Relaxation

Figure 4 shows the variation of the shock-wave angle and certain surface quantities as functions of the nondimensional surface distance x for case I. The results of the modified integral method (solid curves) are seen to vary smoothly from the frozen-flow values behind a frozen shock wave to the equilibrium-flow values behind an equilibrium shock wave (tick mark labeled eq). However, the proper nonequilibrium asymptotes (the entropy layer) for the surface vibrational energy and surface temperature are obtained from the corrected equations (46) and (47). These results are given as solid lines with C's through them in figures 4(c) and (d). Note that to the scale used these are also the corrected results for the standard integral method. It can be seen that the agreement with the characteristics computation (circles) of reference 5 is excellent. The perturbation results of reference 9 (hatched line) are not as accurate as either the modified or the three-strip standard integral results. The erroneous overshoots or undershoots in the asymptotic value of the surface vibrational energy (which are obtained in all approximations of the standard method) do not appear in the modified results.

The variation of the nonequilibrium weighting functions with x is shown in figure 5. It can be seen that these functions monotonically decrease from the tip value of 1/2 toward zero as x increases.

Sedney (ref. 15) points out that, far from the tip, equilibrium flow is inconsistent with the frozen shock-wave boundary condition and also notes the analogy to viscous boundary-layer theory, where inviscid flow is inconsistent with the no-slip surface velocity condition. It can be seen that neither characteristics nor the standard integral method results for the shock-wave angle and surface pressure (figs. 4(a) and (b)) exactly approach the equilibrium

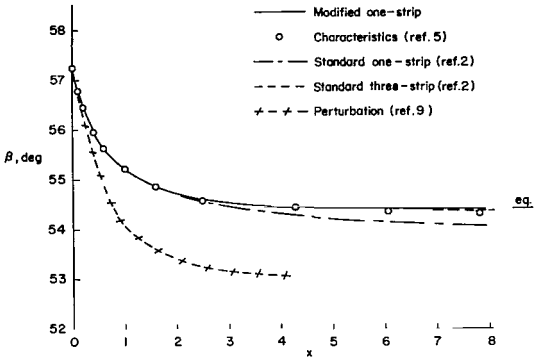

(a) Shock-wave angle as a function of x.

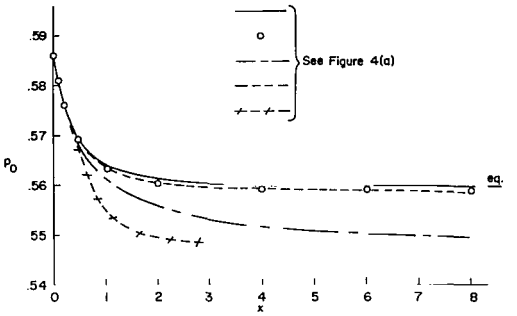

(b) Surface pressure as a function of x.

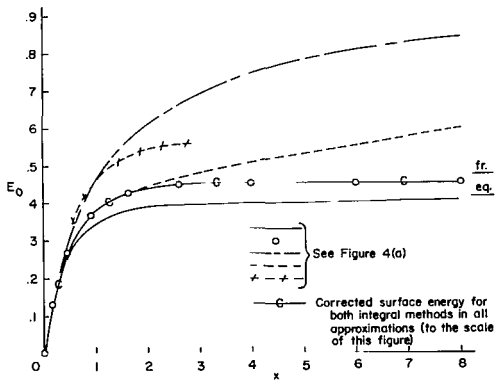

(c) Vibrational energy on surface as a function of x.

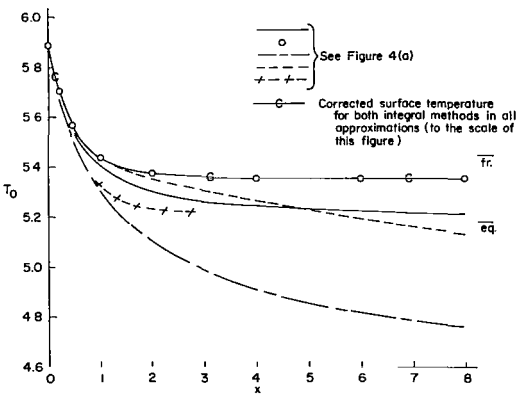

(d) Surface temperature as a function of x.

Figure 4.- Nonequilibrium vibrational flow over a wedge. Case I.

value. In the formulation of the standard integral method this frozen boundary condition is assigned a definite weight (with respect to the entire shock layer) which is not altered far downstream. The method of characteristics would properly weight the frozen boundary condition if the tip region mesh size could be maintained. This procedure is not practical, however, if results far downstream are desired. Thus, in both of these methods, the frozen boundary condition is not properly weighted far downstream. The present modified integral method weights the boundary condition so that its effect far downstream does not disturb the major portion of the shock layer which is in equilibrium. In this method the tip-region relaxation zone is taken to be representative of the relaxation zone behind the shock at all values of x and a small step size is used in the tip region.

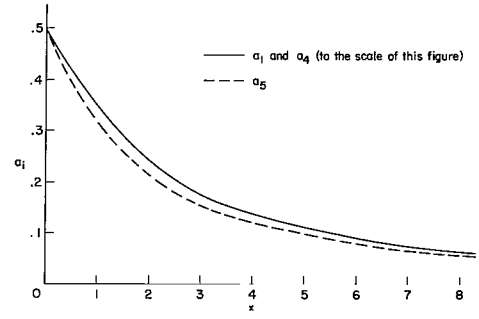

Figure 5.- Variation of the weighting functions for nonequilibrium vibrational flow over a wedge. Case I.

Dissociation Relaxation

Figure 6 shows the variation of the shock-wave angle and certain surface quantities as functions of the nondimensional surface distance x for case II. Again it is seen that the modified integral results (solid curves) vary smoothly from the frozen-flow values behind a frozen shock wave to the equilibrium-flow values behind an equilibrium shock wave (tick mark labeled eq). In figure 6(d), however, only the corrected temperature is plotted. The circles in figure 6 are the characteristics results of reference 7. The curves with long and short dashes in figure 6 give the results of the one-strip standard method.

In determining the weighting functions, frozen conditions behind a frozen-flow shock wave were used since this is the condition in the tip region. However, beyond about one length scale downstream, the shock-wave angle is very close to that for equilibrium flow. In order to see whether or not the frozen and equilibrium geometries give different results, the latter was also used for determining the weighting functions in case II. These results are given in figure 6 as dashed curves. The differences between the frozen- and equilibrium-geometry results are practically negligible. The weighting functions themselves as determined for both situations are plotted as a function of x in figure 7. Again it is seen that they decrease monotonically (with increasing x) toward zero.

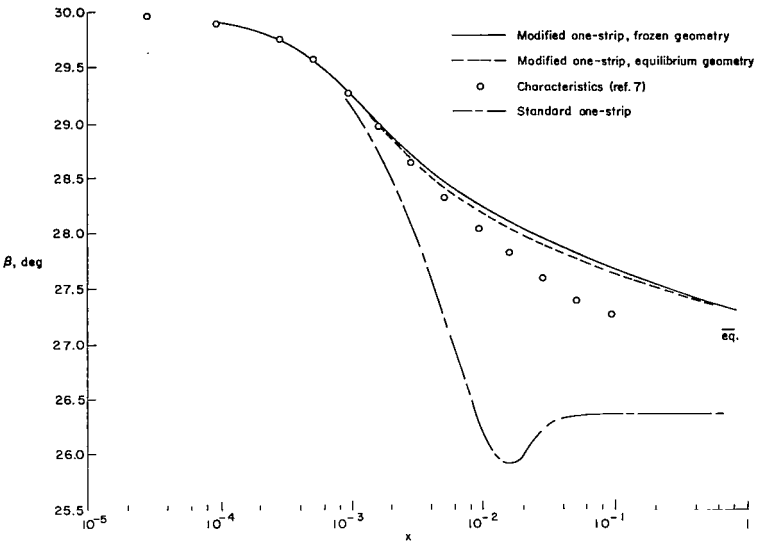

(a) Shock-wave angle as a function of x.

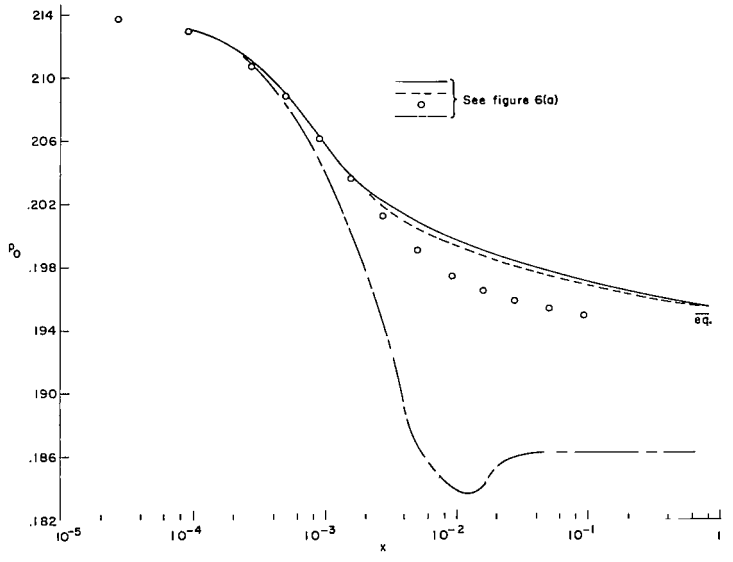

(b) Surface pressure as a function of x.

Figure 6.- Nonequilibrium flow of Lighthill-Freeman "ideal dissociating gas" over a wedge. Case II.

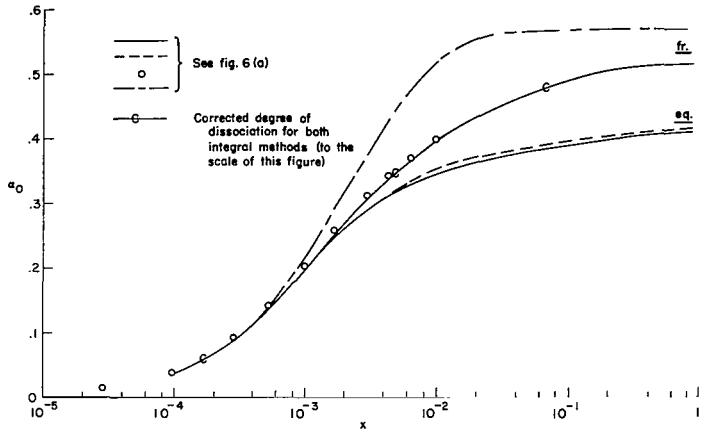

(c) Degree of dissociation on surface as a function of x.

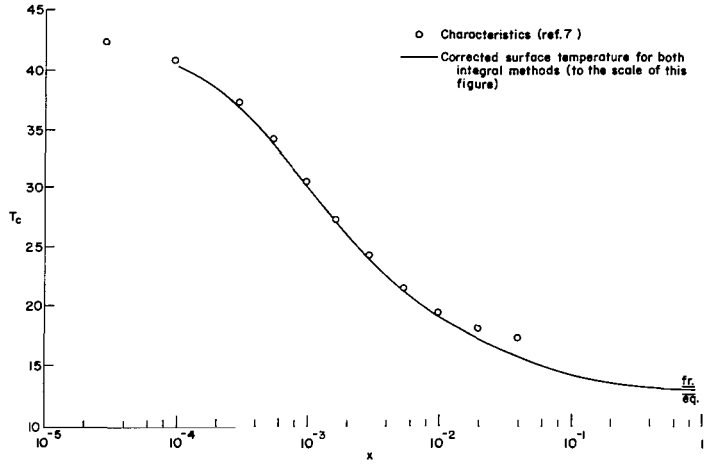

(d) Corrected surface temperature as a function of x.

Figure 6.- Concluded.

As was stated previously, reference 5 shows that the constant-velocity assumption (used herein only in determining the weighting functions) gave results which compared favorably with the characteristics results for vibrational relaxation. Figure 8 shows the effect of this same assumption on the degree of dissociation and temperature for case II (dissociation relaxation). The curve labeled W is for the constant-velocity assumption while the curve labeled C gives the corrected value of the degree of dissociation. The values of T_W and T_C appear to be the same; they differed by less than 1 percent over the entire integration. Thus, the constant-velocity assumption appears to give fairly good results for the variation of temperature and degree of dissociation along the wedge surface.

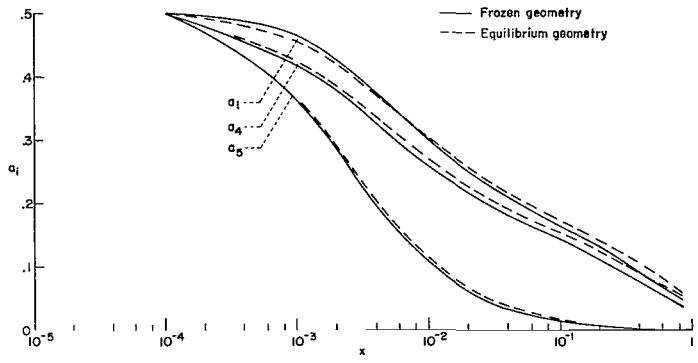

Figure 7.- Variation of the weighting functions for nonequilibrium flow of Lighthill-Freeman "ideal dissociating gas" over a wedge. Case II.

From figures 4 and 6 it can be seen that the asymptotic agreement between the modified and characteristics methods is not as good in case II as in case I. It is believed that the integral results are more nearly correct far downstream. An entropy layer exists on the surface and the manner in which an upper bound for the nonequilibrium asymptotes such as surface temperature and energy should be computed is not known. For the cases considered it appears that the equilibrium condition behind the frozen-flow shock wave gives upper bounds (this corresponds then to an equilibrium shock layer for a larger wedge). The tick marks labeled fr in figures 4(c) and (d) and 6(c) and (d) give the surface vibrational energy (or degree of dissociation) and the temperature for equilibrium conditions behind the frozen-flow shock wave. The lower limits for these two quantities are the equilibrium values behind an equilibrium-flow shock wave and are given as the tick marks labeled eq in figures 4(c) and (d) and 6(c) and (d).

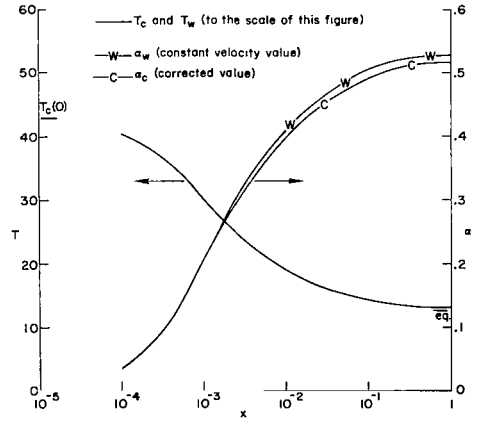

Figure 8.- Comparison of surface temperature and degree of dissociation used in determining weighting functions with the corrected quantities.

It is seen from figures 4(c) and (d) that asymptotic results computed for gas I by the characteristics method (ref. 5) and

both integral methods (when corrected) are bounded by the fr and eq tick marks. However, for gas II it appears from figure 6(d) that the temperature asymptote for the characteristics computation (ref. 7) will not fall between these marks as does the corrected temperature obtained from the integral methods. Since the asymptotic values of all flow variables are interdependent, other asymptotic values given in reference 7 may also be questioned. In reference 5, it is pointed out that when the method of characteristics is used to compute nonequilibrium flows, care must be exercised in the choice of both the finite difference scheme and the dependent variables. In fact, it was found that the standard difference technique was not successful in such a computation. Sedney and Gerber (ref. 6) point out that Capiaux and Washington in reference 16 (essentially a preprint of ref. 7) seem to be using the standard difference technique, but not in Cartesian coordinates. Nothing in reference 7 indicates that the finite difference scheme used in reference 16 has been modified, even though improved results are obtained in reference 7.

The dissociation relaxation case computed by Lee (ref. 9) using the perturbation method appears to be very unrealistic. In order to get a small perturbation, the parameter ρ_D/ρ_∞ was set to about 10^3. Lighthill (ref. 10) points out that for atmospheric values of density, ρ_D/ρ_∞ is at least 10^5.

CONCLUSIONS

The standard method of integral relations has been modified to obtain a better asymptotic behavior.

Specific conclusions which can be drawn are:

1. The modified integral method results vary smoothly from frozen conditions behind a frozen-flow shock wave to equilibrium surface conditions behind an equilibrium-flow shock wave.

2. The nonequilibrium surface entropy layer effects are obtained by defining corrected variables from the exact surface momentum and rate equations.

3. For flow over a wedge, it appears that an upper-bound for certain nonequilibrium surface entropy layer effects is obtained from the equilibrium condition behind a frozen-flow shock wave.

4. A stable integration of the approximate set of ordinary differential equations (obtained from hyperbolic partial differential equations) results only if the integration step size is limited by a stability criterion which is related to the characteristic curves.

5. Computation of the weighting functions for a wedge is easy; for more complex bodies this computation will be more difficult since certain simplifying assumptions cannot be made.

Langley Research Center,
National Aeronautics and Space Administration,
Langley Station, Hampton, Va., November 5, 1964.

APPENDIX A

FROZEN-FLOW SHOCK-WAVE RELATIONS

The required frozen-flow shock-wave relations are taken from reference 14.

Define

$$A \equiv \frac{2}{(\gamma + 1)M_\infty{}^2}\left(M_\infty{}^2\sin^2\beta - 1\right) \tag{A1}$$

then

$$u_\delta = (1 - A)\cos\theta + A\cot\beta\sin\theta \tag{A2}$$

$$v_\delta = -(1 - A)\sin\theta + A\cot\beta\cos\theta \tag{A3}$$

$$\rho_\delta = \frac{(\gamma + 1)M_\infty{}^2\sin^2\beta}{(\gamma - 1)M_\infty{}^2\sin^2\beta + 2} \tag{A4}$$

$$p_\delta = A + \frac{1}{\gamma M_\infty{}^2} \tag{A5}$$

The β derivatives of equations (A2) to (A5) are also needed in order to obtain the β derivatives of the quantities defined in equations (25).

$$\frac{du_\delta}{d\beta} = -\frac{4}{\gamma + 1}\cos\beta\sin\lambda - \frac{A\sin\theta}{\sin^2\beta} \tag{A6}$$

$$\frac{dv_\delta}{d\beta} = \frac{4}{\gamma + 1}\cos\beta\cos\lambda - \frac{A\cos\theta}{\sin^2\beta} \tag{A7}$$

$$\frac{d\rho_\delta}{d\beta} = \frac{4\rho_\delta{}^2\cot\beta}{(\gamma + 1)M_\infty{}^2\sin^2\beta} \tag{A8}$$

$$\frac{dp_\delta}{d\beta} = \frac{4}{\gamma + 1} \sin \beta \cos \beta \tag{A9}$$

then, for example

$$\frac{dt_\delta}{d\beta} = \rho_\delta \frac{du_\delta}{d\beta} + u_\delta \frac{d\rho_\delta}{d\beta} \tag{A10}$$

APPENDIX B

COMPUTATIONAL EQUATIONS

Equations (21) to (24), respectively, are written (by using equation (11)) as:

$$\delta\left(1 - a_1\right)\frac{dt_0}{dx} + \delta a_1 \frac{dt_\delta}{d\beta}\frac{d\beta}{dx} = K_1 \tag{B1}$$

$$\delta\left(1 - a_2\right)\frac{dg_0}{dx} + \delta a_2 \frac{dg_\delta}{d\beta}\frac{d\beta}{dx} = K_2 \tag{B2}$$

$$\delta a_3 \frac{dz_\delta}{d\beta}\frac{d\beta}{dx} = K_3 \tag{B3}$$

$$\delta\left(1 - a_4\right)\left[t_0 \frac{dE_0}{dx} + E_0 \frac{dt_0}{dx}\right] = K_{4I} \tag{B4.I}$$

$$\delta\left(1 - a_4\right)\left[t_0 \frac{d\alpha_0}{dx} + \alpha_0 \frac{dt_0}{dx}\right] = K_{4II} \tag{B4.II}$$

where

$$K_1 \equiv -\left\{\left(1 - a_1\right)\left(t_0 - t_\delta\right)\tan\lambda + h_\delta - \delta\left(t_0 - t_\delta\right)\frac{da_1}{dx}\right\} \tag{B5}$$

$$K_2 \equiv -\left\{\left(1 - a_2\right)\left(g_0 - g_\delta\right)\tan\lambda + z_\delta - \delta\left(g_0 - g_\delta\right)\frac{da_2}{dx}\right\} \tag{B6}$$

$$K_3 \equiv -\left\{-\left(1 - a_3\right)z_\delta \tan\lambda + H_\delta - p_0 + \delta z_\delta \frac{da_3}{dx}\right\} \tag{B7}$$

$$K_{4I} = -\left\{\left(1 - a_4\right)t_0E_0 \tan\lambda - \delta\left[\left(1 - a_5\right)\rho_0\epsilon_0 + a_5\rho_\delta\epsilon_\delta + t_0E_0\frac{da_4}{dx}\right]\right\} \tag{B8.I}$$

$$K_{4II} = -\left\{\left(1 - a_4\right)t_0\alpha_0 \tan\lambda - \delta\left[\left(1 - a_5\right)\rho_0\phi_0 + a_5\rho_\delta\phi_\delta + t_0\alpha_0\frac{da_4}{dx}\right]\right\} \tag{B8.II}$$

Equation (B3) gives $d\beta/dx$ as

$$\frac{d\beta}{dx} = \frac{K_3}{\delta a_3\left(\frac{dz_\delta}{d\beta}\right)} \tag{B9}$$

Equations (B1), (B4), and (B9) give the rate equation for gases I and II, respectively, as

$$\frac{dE_0}{dx} = \frac{1}{\delta t_0\left(1 - a_4\right)}\left\{K_{4I} - E_0\frac{\left(1 - a_4\right)}{\left(1 - a_1\right)}\left[K_1 - \frac{a_1\frac{dt_\delta}{d\beta}}{a_3\frac{dz_\delta}{d\beta}}K_3\right]\right\} \tag{B10.I}$$

$$\frac{d\alpha_0}{dx} = \frac{1}{\delta t_0\left(1 - a_4\right)}\left\{K_{4II} - \alpha_0\frac{\left(1 - a_4\right)}{\left(1 - a_1\right)}\left[K_1 - \frac{a_1\frac{dt_\delta}{d\beta}}{a_3\frac{dz_\delta}{d\beta}}K_3\right]\right\} \tag{B10.II}$$

In order to separate the differential equations for p_0 and u_0, the energy and state equations ((5) and (6)) must be differentiated and used with (B1) to (B4). For gas I, these separated equations are

$$\frac{du_0}{dx} = \frac{1}{\delta t_0\left(M_0^2 - 1\right)}\left\{\frac{\frac{7}{5}M_0^2}{\left(1 - a_2\right)}\left[K_2 - \frac{a_2\frac{dg_\delta}{d\beta}}{a_3\frac{dz_\delta}{d\beta}}K_3\right] + \frac{u_0 K_{4I}}{\left(1 - a_4\right)T_0}\right.$$

$$\left. - \frac{u_0}{\left(1 - a_1\right)}\left(\frac{7}{5}M_0^2 + 1 + \frac{E_0}{T_0}\right)\left[K_1 - \frac{a_1\frac{dt_\delta}{d\beta}}{a_3\frac{dz_\delta}{d\beta}}K_3\right]\right\} \qquad \text{(B11.I)}$$

$$\frac{dp_0}{dx} = \frac{-1}{\delta\left(M_0^2 - 1\right)}\left\{\frac{\left(1 + \frac{2}{5}M_0^2\right)}{\left(1 - a_2\right)}\left[K_2 - \frac{a_2\frac{dg_\delta}{d\beta}}{a_3\frac{dz_\delta}{d\beta}}K_3\right] + \frac{u_0 K_{4I}}{\left(1 - a_4\right)T_0}\right.$$

$$\left. - \frac{u_0}{\left(1 - a_1\right)}\left(2 + \frac{2}{5}M_0^2 + \frac{E_0}{T_0}\right)\left[K_1 - \frac{a_1\frac{dt_\delta}{d\beta}}{a_3\frac{dz_\delta}{d\beta}}K_3\right]\right\} \qquad \text{(B12.I)}$$

where M_0, the frozen-flow Mach number on the surface, is given by

$$M_0 = M_\infty \frac{u_0}{\sqrt{T_0}} \qquad \text{(B13.I)}$$

For gas II, the corresponding equations are

$$\frac{du_0}{dx} = \frac{1}{\delta t_0\left(A_1 t_0 - A_3\right)}\left\{\frac{A_1 t_0}{\left(1 - a_2\right)}\left[K_2 - \frac{a_2\frac{dg_\delta}{d\beta}}{a_3\frac{dz_\delta}{d\beta}}K_3\right] + \frac{A_2 K_{4II}}{\left(1 - a_4\right)}\right.$$

$$\left. - \left[\frac{A_2\alpha_0 + t_0\left(A_1 + 1\right)u_0}{\left(1 - a_1\right)}\right]\left[K_1 - \frac{a_1\frac{dt_\delta}{d\beta}}{a_3\frac{dz_\delta}{d\beta}}K_3\right]\right\} \qquad \text{(B11.II)}$$

$$\frac{dp_0}{dx} = \frac{-1}{\delta\left(A_1 t_0 - A_3\right)} \left\{ \frac{A_3}{\left(1 - a_2\right)} \left[K_2 - \frac{a_2 \frac{dg_\delta}{d\beta}}{a_3 \frac{dz_\delta}{d\beta}} K_3 \right] + \frac{A_2 K_{4II}}{\left(1 - a_4\right)} \right.$$

$$\left. - \left[\frac{A_2 \alpha_0 + \left(A_3 + t_0\right) u_0}{\left(1 - a_1\right)} \right] \left[K_1 - \frac{a_1 \frac{dt_\delta}{d\beta}}{a_3 \frac{dz_\delta}{d\beta}} K_3 \right] \right\} \qquad \text{(B12.II)}$$

$$M_0 = M_\infty \frac{u_0}{\sqrt{\left(1 + \alpha_0\right)\left(1 + \frac{\alpha_0}{4}\right) T_0}} \qquad \text{(B13.II)}$$

where

$$\left.\begin{aligned} A_1 &\equiv \frac{u_0 t_0}{p_0} \\ A_2 &\equiv \frac{u_0 t_0}{T_0} \left[\frac{K\left(1 + \alpha_0\right) - 3T_0}{\left(4 + \alpha_0\right)\left(1 + \alpha_0\right)} \right] \\ A_3 &\equiv t_0 \left[\frac{4 M_\infty{}^2 u_0{}^2}{3\left(4 + \alpha_0\right) T_0} + 1 \right] \end{aligned}\right\} \qquad \text{(B14.II)}$$

APPENDIX C

INITIAL WEIGHTING FUNCTIONS

In order to obtain the initial values of a_i, the behavior of $\bar{Q}_i$ for small x must be determined. The Maclaurin expansion for $Q_{i,w}\left(= Q_{i,0}\right)$ is

$$Q_{i,w}(x) = Q_{i,W} + \left(\frac{dQ_{i,w}}{dx}\right)_0 x + \text{Order}\left(x^2\right) \tag{C1}$$

Then for a small step Δx away from the origin, first-order integration of equation (32) gives

$$\bar{Q}_i(\Delta x) \approx Q_{i,W} + \left(\frac{dQ_{i,w}}{dx}\right)_0 \frac{\Delta x}{2} \tag{C2}$$

But

$$\left(\frac{dQ_{i,w}}{dx}\right)_0 \approx \frac{Q_{i,w}(\Delta x) - Q_{i,W}}{\Delta x} \tag{C3}$$

thus

$$\bar{Q}_i(\Delta x) \approx \frac{1}{2}\left[Q_{i,W} + Q_{i,w}(\Delta x)\right] \tag{C4}$$

It can be seen from equations (C4) and (33) or (34) that

$$a_i(\Delta x) \approx \frac{1}{2} \tag{C5}$$

irrespective of whether $Q_{i,W} = 0$ or not. Thus

$$a_i(0) = \frac{1}{2} \tag{C6}$$

Had only the first term of equation (C1) been used, $a_i(0)$ would have been found to be indeterminate; thus the second term is needed.

APPENDIX D

INITIAL DERIVATIVES

The $\lim_{x \to 0} \left(\frac{K_i}{\delta}\right)$ obtained from equations (B5) to (B8), the boundary conditions, and frozen initial solution (appendixes A and C) is

$$\left(\frac{K_1}{\delta}\right)_0 = -\left\{\frac{1}{2}\left[\left(\frac{dt_0}{dx}\right)_0 - \frac{dt_\delta}{d\beta}\left(\frac{d\beta}{dx}\right)_0\right] + \cot\lambda \frac{dh_\delta}{d\beta}\left(\frac{d\beta}{dx}\right)_0\right\} \tag{D1}$$

$$\left(\frac{K_2}{\delta}\right)_0 = -\left\{\frac{1}{2}\left[\left(\frac{dg_0}{dx}\right)_0 - \frac{dg_\delta}{d\beta}\left(\frac{d\beta}{dx}\right)_0\right] + \cot\lambda \frac{dz_\delta}{d\beta}\left(\frac{d\beta}{dx}\right)_0\right\} \tag{D2}$$

$$\left(\frac{K_3}{\delta}\right)_0 = -\left\{-\frac{1}{2}\frac{dz_\delta}{d\beta}\left(\frac{d\beta}{dx}\right)_0 + \cot\lambda\left[\frac{dH_\delta}{d\beta}\left(\frac{d\beta}{dx}\right)_0 - \left(\frac{dp_0}{dx}\right)_0\right]\right\} \tag{D3}$$

$$\left(\frac{K_{4I}}{\delta}\right)_0 = -\left\{\frac{1}{2}\, t_\delta\left(\frac{dE_0}{dx}\right)_0 - \rho_\delta \epsilon_\delta\right\} \tag{D4.I}$$

$$\left(\frac{K_{4II}}{\delta}\right)_0 = -\left\{\frac{1}{2}\, t_\delta\left(\frac{d\alpha_0}{dx}\right)_0 - \rho_\delta \phi_\delta\right\} \tag{D4.II}$$

Equations (B1) to (B4) become after multiplying by $1/\delta$, taking $\lim_{x \to 0}$, and applying the initial solution

$$\frac{1}{2}\left[\left(\frac{dt_0}{dx}\right)_0 + \frac{dt_\delta}{d\beta}\left(\frac{d\beta}{dx}\right)_0\right] = \left(\frac{K_1}{\delta}\right)_0 \tag{D5}$$

$$\frac{1}{2}\left[\left(\frac{dg_0}{dx}\right)_0 + \frac{dg_\delta}{d\beta}\left(\frac{d\beta}{dx}\right)_0\right] = \left(\frac{K_2}{\delta}\right)_0 \tag{D6}$$

$$\frac{1}{2}\frac{dz_\delta}{d\beta}\left(\frac{d\beta}{dx}\right)_0 = \left(\frac{K_3}{\delta}\right)_0 \tag{D7}$$

$$\frac{1}{2}t_\delta\left(\frac{dE_0}{dx}\right)_0 = \left(\frac{K_{4I}}{\delta}\right)_0 \tag{D8.I}$$

$$\frac{1}{2}t_\delta\left(\frac{d\alpha_0}{dx}\right)_0 = \left(\frac{K_{4II}}{\delta}\right)_0 \tag{D8.II}$$

With equation (D4) substituted into equation (D8), $\left(\frac{dE_0}{dx}\right)_0$ and $\left(\frac{d\alpha_0}{dx}\right)_0$ are given as

$$\left(\frac{dE_0}{dx}\right)_0 = \frac{\epsilon_\delta}{u_\delta} \tag{D9.I}$$

$$\left(\frac{d\alpha_0}{dx}\right)_0 = \frac{\phi_\delta}{u_\delta} \tag{D9.II}$$

As was the case in appendix B, the energy and state equations ((5) and (6)) must be used with equations (D1) to (D9) in order to separate the other differentials. These initial derivatives for gas I are then

$$\left(\frac{d\beta}{dx}\right)_0 = \frac{-t_\delta\epsilon_\delta}{T_\delta\left[\left(M_\delta^2 - 1\right)\frac{dp_\delta}{d\beta} + t_\delta \cot\lambda \frac{dv_\delta}{d\beta}\right]} \tag{D10.I}$$

$$\left(\frac{dp_0}{dx}\right)_0 = \frac{dp_\delta}{d\beta}\left(\frac{d\beta}{dx}\right)_0 \tag{D11.I}$$

$$\left(\frac{du_0}{dx}\right)_0 = -\frac{1}{t_\delta}\left(\frac{dp_0}{dx}\right)_0 \tag{D12.I}$$

These equations are identical to those obtained by South in reference 3. For gas II, the corresponding initial derivatives are

$$\left(\frac{d\beta}{dx}\right)_0 = \frac{-t_\delta\left(K - 3T_\delta\right)\phi_\delta}{4T_\delta\left[\left(M_\delta{}^2 - 1\right)\frac{dp_\delta}{d\beta} + t_\delta \cot \lambda \frac{dv_\delta}{d\beta}\right]} \tag{D10.II}$$

$$\left(\frac{dp_0}{dx}\right)_0 = \frac{dp_\delta}{d\beta}\left(\frac{d\beta}{dx}\right)_0 \tag{D11.II}$$

$$\left(\frac{du_0}{dx}\right)_0 = -\frac{1}{t_\delta}\left(\frac{dp_0}{dx}\right)_0 \tag{D12.II}$$

REFERENCES

1. Belotserkovskiy, O. M.; and Chushkin, P. I.: The Numerical Method of Integral Relations. Zhurnal vychislitel'noy matematiki i matematicheskoy fiziki (J. Computational Mathematics and Mathematical Physics), vol. II, no. 5, Moscow, Sept.-Oct. 1962, pp. 731-759. Also available as NASA TT F-8356.

2. South, J. C., Jr.: Application of the Method of Integral Relations to Supersonic Nonequilibrium Flow Past Wedges and Cones. NASA TR R-205, 1964.

3. South, Jerry C., Jr.: Application of Dorodnitsyn's Integral Method to Nonequilibrium Flows Over Pointed Bodies. NASA TN D-1942, 1963.

4. Shih, William C. L.; Baron, Judson R.; Krupp, Roy S.; and Towle, William J.: Nonequilibrium Blunt Body Flow Using the Method of Integral Relations. Tech. Rept. 66 (Contract NOw 62-0765-d), Aerophys. Lab., M.I.T., May 1963. (Available from DDC as 415934.)

5. Sedney, R.; South, J. C.; and Gerber, N.: Characteristic Calculation of Non-Equilibrium Flows. Rept. No. 1173, Ballistic Res. Labs., Aberdeen Proving Ground, Apr. 1962.

6. Sedney, R.; and Gerber, N.: Nonequilibrium Flow Over a Cone. AIAA J., vol. 1, no. 11, Nov. 1963, pp. 2482-2486.

7. Capiaux, R.; and Washington, M.: Nonequilibrium Flow Past a Wedge. AIAA J., vol. 1, no. 3, Mar. 1963, pp. 650-660.

8. Wood, A. D.; Springfield, J. F.; and Pallone, A. J.: Determination of the Effects of Chemical and Vibrational Relaxation on an Inviscid Hypersonic Flow Field. RAD-TM-63-88 (Contract AF04(694)-239), AVCO Res. and Advanced Develop. Div. Corp., Jan. 22, 1964.

9. Lee, Richard S.: A Study of Supersonic Nonequilibrium Flow Over a Wedge. SUDAER-160, Stanford Univ., June 1963.

10. Lighthill, M. J.: Dynamics of a Dissociating Gas - Part I Equilibrium Flow. J. Fluid Mech., vol. 2, pt. I, Jan. 1957, pp. 1-32.

11. Freeman, N. C.: Dynamics of a Dissociating Gas - Part III. Non-Equilibrium Theory. Rept. 133, AGARD, North Atlantic Treaty Organization (Paris), Jul. 1957.

12. Blackman, Vernon: Vibrational Relaxation in Oxygen and Nitrogen. J. Fluid Mech., vol. 1, pt. 1, May 1956, pp. 61-85.

13. Matthews, D. L.: Interferometric Measurement in the Shock Tube of the Dissociation Rate of Oxygen. Phys. Fluids, vol. 2, no. 2, Mar.-Apr. 1959, pp. 170-178.

14. Ames Research Staff: Equations, Tables, and Charts for Compressible Flow. NACA Rep. No. 1135, 1953. (Supersedes NACA TN 1428.)

15. Sedney, Raymond: Some Aspects of Nonequilibrium Flows. J. Aerospace Sci., vol. 28, no. 3, Mar. 1961, pp. 189-196, 208.

16. Capiaux, R.; and Washington, M.: Non-Equilibrium Flow Past a Wedge. IAS Paper No. 62-99, June 19-22, 1962.

NASA-Langley, 1965 L-4187

"The aeronautical and space activities of the United States shall be conducted so as to contribute . . . to the expansion of human knowledge of phenomena in the atmosphere and space. The Administration shall provide for the widest practicable and appropriate dissemination of information concerning its activities and the results thereof."

—NATIONAL AERONAUTICS AND SPACE ACT OF 1958

NASA SCIENTIFIC AND TECHNICAL PUBLICATIONS

TECHNICAL REPORTS: Scientific and technical information considered important, complete, and a lasting contribution to existing knowledge.

TECHNICAL NOTES: Information less broad in scope but nevertheless of importance as a contribution to existing knowledge.

TECHNICAL MEMORANDUMS: Information receiving limited distribution because of preliminary data, security classification, or other reasons.

CONTRACTOR REPORTS: Technical information generated in connection with a NASA contract or grant and released under NASA auspices.

TECHNICAL TRANSLATIONS: Information published in a foreign language considered to merit NASA distribution in English.

TECHNICAL REPRINTS: Information derived from NASA activities and initially published in the form of journal articles.

SPECIAL PUBLICATIONS: Information derived from or of value to NASA activities but not necessarily reporting the results of individual NASA-programmed scientific efforts. Publications include conference proceedings, monographs, data compilations, handbooks, sourcebooks, and special bibliographies.

Details on the availability of these publications may be obtained from:

SCIENTIFIC AND TECHNICAL INFORMATION DIVISION

NATIONAL AERONAUTICS AND SPACE ADMINISTRATION

Washington, D.C. 20546